Progress In Electromagnetics Research, Vol. 110, 59–80, 2010

TRANSPORT AND ELECTRONIC PROPERTIES OF TWO DIMENSIONAL ELECTRON GAS IN DELTA-MIGFET IN GAAS

O. Oubram †

Instituto de Física
Benemérita Universidad Autónoma de Puebla
Apartado Postal J-48, Puebla, Pue. 72570, México

L. M. Gaggero-Sager

Facultad de Ciencias
Universidad Autónoma del Estado de Morelos
Av. Universidad 1001, Col. Chamilpa
Cuernavaca, Morelos CP 62209, México

A. Bassam

Centro de Investigación en Energía
Universidad Nacional Autónoma de México
Privada Xochicalco s/n, Centro, Temixco, Morelos 62580, México

G. A. Luna-Acosta

Instituto de Física
Benemérita Universidad Autónoma de Puebla
Apartado Postal J-48, Puebla, Pue. 72570, México

Abstract—The objective of this work is to analyze electronic transport phenomena, due to ionized impurity scattering in δ-MIGFET (Delta-Multiple Independent Gate Field Effect Transistor). In this work, we report theoretical results for electronic transport in a delta-MIGFET using the device electronic structure and analytical expression of mobility and conductivity. The results show that the analytical mobility and conductivity are a good way to analyze

Received 13 August 2010, Accepted 14 October 2010, Scheduled 10 November 2010
Corresponding author: Outmane Oubram (oubram@uaem.mx).
† Also with Instituto de Investigaciones en Materiales, Universidad Nacional Autónoma de México, Apartado Postal 70-360, México D.F 04510, México.

transport in this device. We find the relative mobility as a linear and increasing function in different modes; also, we find transconductance as an almost flat function in all the evaluated interval. Finally, we analyze the differential capacitance and resistivity, and we report regions where this device is operating in digital and analogue mode. These regions are delimited in terms of intrinsic and extrinsic parameters of this device in symmetrical mode.

1. INTRODUCTION

Rapid and predictable scaling of planar CMOS devices is becoming difficult. Recently, it is very hard to conserve MOORE's law with the conventional microelectronics technology, and it needs to search a new alternative [1–5].

Now some new devices appear to replace the planar CMOS devices. These are subject to investigations using multiple surfaces and are promising to improve scaling and could even make new circuits feasible, to achieve better characteristics [6–10].

Double gate Silicon On Insulator (SOI) devices have been also widely researched to replace the current planar SOI devices [8, 11, 12]. The main advantage of this architecture is that it offers a reinforced electrostatic coupling between the conduction channel and the gate electrode. A double gate structure can efficiently sandwich the semiconductor element playing the role of the transistor channel [13]. Recently, double gate structures with independent gate devices have offered additional advantages and challenges [2, 6, 14–17].

We introduce a new device with double gate and 2DEG (Two-Dimensional Electron Gas) as conduction channel δ-MIGFET (δ-Multiple Independent Gate FET) (Figure 1), where double gate electrodes control a delta-doped channel using double gate electrodes that are separated from each other.

Mainly, we will study the transport properties of the new δ-MIGFET (δ-Multiple Independent Gate FET) (Figure 1) transistor in symmetrical and asymmetrical modes. The transconductance observed in this system is almost stable in asymmetrical mode as the experimental work in conventional MIGFET [11]. This feature is highly desirable in electronics to reduce the noise in amplifications and improve the stability [18].

Furthermore, we have also found that the mobility is more linear in the asymmetrical mode than in the symmetrical one and that it doubles when the contact potentials are high, allowing a better performance [19, 20].

These properties are due primarily to the good electronic

confinement achieved in the two contact gates on both sides and secondly, to the conduction channel control in an independent way in the two gates.

The transport phenomena is studied in two forms. The first one requires the electronic structure calculations results, as a preview study applied to δ-FET and ALD-FET [21–23]. The second one uses the Thomas Fermi approach; this one has an advantage since it is not necessary to calculate the electronic structure [eigenfunctions, eigenvalues].

Finally we present the relative analytical resistivity. It is noted that it has an almost linear behaviors and depends on the density of the confined electrons. We specify the regions of operation in analog and digital systems and present the relative differential capacity of the system. It has been shown that the behavior of the capacity mainly depends on the density of the doped delta that is comparable of the work reported in other systems [24, 25].

2. THEORETICAL BACKGROUND

The δ-MIGFET is a conventional MIGFET [6, 7] with a delta doped as the conduction channel. The δ-doping technique allows one to obtain an extremely sharp doping profile and a high-density-doped layer [26–29], and it is of great interest [30–32].

The potential of this system is formed by a first metal-semiconductor contact (Schottky barrier), followed by the n-type delta-doped quantum-well system and second metal-semiconductor contact (Schottky barrier) (Figure 1). The presence of a confined electronic gas depends on the parameters used in the construction of the system.

If there is electronic confinement, the model for describing the conduction band of the semiconductor in the δ-MIGFET system has, as a main assumptions, the potential profile described by the depletion

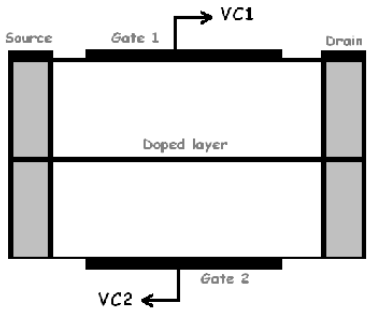

Figure 1. Cross-section of Delta-MIGFET in GaAs.

region approach in the proximity of the first metal-semiconductor contact [33].

$$V_{dep}(z) = \frac{2\pi e^2}{\epsilon_r} N_d (z + d - l)^2. \tag{1}$$

where N_d is the background impurity density; ϵ_r is the electric permittivity constant of GaAs; $-d$ (d) is the distance at which the first (second) gate is positioned, respectively; and l is the screening distance for the electric field.

$$l = \sqrt{\frac{\epsilon_r V_{c1}}{2\pi e^2 N_d}}. \tag{2}$$

Here V_{c1} is the first contact voltage.

The second assumption is that, in the region not too close to the interface, the delta-doped well potential is described within a self-consistent Thomas-Fermi approach by:

$$V_n(z) - E_f = -\frac{\alpha_n^2}{(\alpha_n |z| + z_{0n})^4}, \tag{3}$$

$\alpha_n = 2/(15\pi)$ and $z_{0n} = (\alpha_n^3/\pi N_{2d})^{1/5}$, is the distance at which the n-type delta-doped well is positioned. N_{2d} is the two-dimensional impurity density of the n-type delta-doped quantum-well, and E_f is the Fermi level.

The third potential describes the depletion region approach in the proximity of the second metal-semiconductor contact.

$$V_{dep}^{'}(z) = \frac{2\pi e^2}{\epsilon_r} N_d (z - d + l^{'})^2, \tag{4}$$

$l^{'}$ is the screening distance for the electric field, where

$$l^{'} = \sqrt{\frac{\epsilon_r V_{c2}}{2\pi e^2 N_d}}. \tag{5}$$

Here V_{c2} is the second contact voltage.

The entire potential is then,

$$\begin{aligned} V(z) = {} & \frac{2\pi e^2}{\epsilon_r} N_d (z+d-l)^2 \theta(-d+l-z) - \frac{\alpha_n^2}{(\alpha_n |z| + z_{0n})^4} \theta(z - l_p) \theta(l_p^{'} - z) \\ & + \frac{2\pi e^2}{\epsilon_r} N_d (z - d + l')^2 \theta(z - d + l'). \end{aligned} \tag{6}$$

where l_p ($l_p^{'}$) is the first (the second) depletion region width, $V(l_p) = 0$ ($V(l_p^{'}) = 0$). We have assumed that the Fermi level E_f is close to the conduction band. θ is the unit-step function.

We will calculate eigenvalues and eigenfunctions for the following section, with (6) and Schrödinger equation:

$$-\frac{\hbar^2}{2m_e^*}\frac{d^2F_i(z)}{dz^2}+V(z)F_i(z)=E_iF_i(z) \tag{7}$$

where $F_i(z)$ (E_i) is the ith eigenfunction (eigenvalue) of n-type delta-doped respectively.

2.1. Transport Properties

Based on the Thomas Fermi approximation to this δ-MIGFET, we study the electron transport properties of the system. We only consider the ionized donor scattering mechanism, because it is the most important at low temperature. The Coulomb scattering potential due to the ionized impurities is considered as distributed randomly in the doped layer. Finally, we take the ratio of the mobility [34]:

$$\mu_{rel}=\frac{\mu^{V_{c1},V_{c2}}}{\mu^{V_{c1}=0,V_{c2}}}=\frac{\int\int\rho_e^{V_{c1}=0,V_{c2}}(z')\,\rho_{imp}^{V_{c1}=0,V_{c2}}(z)\,|z-z'|dzdz'}{\int\int\rho_e^{V_{c1},V_{c2}}(z')\,\rho_{imp}^{V_{c1},V_{c2}}(z)\,|z-z'|dzdz'}, \tag{8}$$

$\rho_e^{V_{c1},V_{c2}}(z')\left(\rho_e^{V_{c1}=0,V_{c2}}(z')\right)$ is the density of electrons of n-type delta-doped where the first potential contact is V_{c1} ($V_{c1}=0$), and the second potential contact is V_{c2}, respectively;

$\rho_{imp}^{V_{c1},V_{c2}}(z)\left(\rho_{imp}^{V_{c1}=0,V_{c2}}(z)\right)$ is the density of impurities of n-type delta-doped where the first potential contact is V_{c1} ($V_{c1}=0$), and the second potential contact is V_{c2}, respectively.

With $\rho_{imp}^{V_{c1},V_{c2}}=N_{2d}\times\delta(z)$ and $\delta(z)$ is Dirac delta.

Expression (8) can be put in the following form:

$$\mu_{rel}=\frac{\int\rho_e^{V_{c1}=0,V_{c2}}(z)\,|z|dz}{\int\rho_e^{V_{c1},V_{c2}}(z)\,|z|dz}. \tag{9}$$

Using the mass effective theory at $T=0\,\mathrm{K}$:

$$\rho_e(z)=\frac{em^*}{\pi\hbar^2}\Sigma_1^{n_e}|F_i(z)|^2(E_f-E_i)\theta(E_f-E_i), \tag{10}$$

where E_f is the Fermi level; E_i is the ith level of n-type delta-doped; n_e is electronics states number; and θ is the unit-step function.

Using (10) in (9) the expression (8) will be:

$$\mu_{rel}=\frac{\mu^{V_{c1},V_{c2}}}{\mu^{V_{c1}=0,V_{c2}}}=\frac{\Sigma_1^{n_e}\int|F_i^{V_{c1}=0,V_{c2}}(z)|^2\left(E_f^{V_{c1}=0,V_{c2}}-E_i^{V_{c1}=0,V_{c2}}\right)|z|dz}{\Sigma_1^{n_e}\int|F_i^{V_{c1},V_{c2}}(z)|^2\left(E_f^{V_{c1},V_{c2}}-E_i^{V_{c1},V_{c2}}\right)|z|dz}, \tag{11}$$

where $F_i^{V_{c1},V_{c2}}(z)$, $E_f^{V_{c1},V_{c2}}$ and $E_i^{V_{c1},V_{c2}}$ $[F_i^{V_{c1}=0,V_{c2}}(z)$, $E_f^{V_{c1}=0,V_{c2}}$ and $E_i^{V_{c1}=0,V_{c2}}]$ are the envelope functions, the Fermi level and the ith level of n-type delta-doped, respectively, where the first potential contact is V_{c1} ($V_{c1}=0$). The former expression is valid for $T=0\,\mathrm{K}$.

The relative electronic density is defined as

$$n_{rel}=\frac{n^{V_{c1},V_{c2}}}{n^{V_{c1}=0,V_{c2}}}. \tag{12}$$

Finally the relative conductivity is as

$$\sigma_{rel}=n_{rel}\times\mu_{rel}. \tag{13}$$

In this case we need the eigenvalues and eigenfunctions to calculate μ_{rel}, n_{rel} and σ_{rel}.

Now, we introduce the analytical transport:

The expression (10) of $\rho_e(z)$ in the Thomas-Fermi approximation is:

$$\rho_e(z)=\frac{1}{2\pi e^2\hbar^2}(2m^*)^{\frac{3}{2}}(E_f-V(z))^{\frac{3}{2}}, \tag{14}$$

in which it presupposes that there are only electrons in the region classically allowed, then $z\in[l_p,l_p^{'}]$ and $V(z)$ is given by (6).

The analytical relative mobility quantity for (V_{c1},V_{c2}) is defined as:

$$\begin{aligned}\mu_{rel}^{'} &= \frac{\mu^{'V_{c1},V_{c2}}}{\mu^{'V_{c1}=V_{c2}=0\,rmmeV}}\\ &= \frac{\int_{l_p}^{l_p^{'}}\rho_e^{V_{c1}=V_{c2}=0\,\mathrm{meV}}(z)\,\rho_{imp}^{V_{c1}=V_{c2}=0\,\mathrm{meV}}|z-z'|dzdz'}{\int_{l_p}^{l_p^{'}}\rho_e^{V_{c1},V_{c2}}(z)\,\rho_{imp}^{V_{c1},V_{c2}}|z-z'|dzdz'}.\end{aligned} \tag{15}$$

In the first approximation which we will consider only the delta-doped potential effect when $z\in[l_p,l_p^{'}]$ then:

$$V(z)\simeq V_n(z)=-\frac{\alpha_n^2}{(\alpha_n|z|+z_{0n})^4}. \tag{16}$$

Using (9), (14) and (16), $\mu_{rel}^{'}$ will be:

$$\mu_{rel}^{'}=\frac{\left[\int_{l_p}^{l_p^{'}}(E_f-V_n(z))^{\frac{3}{2}}|z|dz\right]^{V_{c1}=V_{c2}=0meV}}{\left[\int_{l_p}^{l_p^{'}}(E_f-V_n(z))^{\frac{3}{2}}|z|dz\right]^{V_{c1},V_{c2}}}, \tag{17}$$

with $l_p<0$, $0<l_p^{'}$, $V(l_p)=V(l_p^{'})=0$ and $E_f=0\,\mathrm{meV}$ in GaAs.

The analytical relative mobility expression may be written as

$$\mu_{rel}^{'} = 2\left[\left(2 - \frac{5l_p - a}{(l_p - a)^5}a^4 - \frac{5l_p^{'} + a}{(l_p^{'} + a)^5}a^4\right)^{-1}\right]^{V_{c1},V_{c2}}, \quad (18)$$

with $a = \frac{z_{0n}}{\alpha_n}$.

When $V_{c1} = V_{c2}$ the analytical relative mobility expression may be written as

$$\mu_{rel}^{'} = \left[\left(1 - \frac{5l_p - a}{(l_p - a)^5}a^4\right)^{-1}\right]^{V_{c1}=V_{c2}}. \quad (19)$$

We define the analytical relative electronic density as

$$n_{rel}^{'} = \frac{\int_{l_p}^{l_p^{'}} \rho_e^{V_{c1},V_{c2}}(z)\,dz}{\int_{l_p}^{l_p^{'}} \rho_e^{V_{c1}=V_{c2}=0\,\mathrm{meV}}(z)\,dz} = \frac{\rho_e^{V_{c1},V_{c2}}}{\rho_e^{V_{c1}=V_{c2}=0\,\mathrm{meV}}}. \quad (20)$$

Using the same approximation as before, we obtain:

$$n_{rel}^{'} = \left[1 + \frac{a^5}{2}\left(\frac{1}{(l_p - a)^5} - \frac{1}{(l_p^{'} + a)^5}\right)\right]^{V_{c1},V_{c2}}. \quad (21)$$

When $V_{c1} = V_{c2}$ the analytical relative density will be:

$$n_{rel}^{'} = \left[1 + \frac{a^5}{(l_p - a)^5}\right]^{V_{c1}=V_{c2}}. \quad (22)$$

Finally, the relative analytical conductivity is

$$\sigma_{rel}^{'} = n_{rel}^{'} \times \mu_{rel}^{'} \quad (23)$$

Using (19) and (22), $\sigma_{rel}^{'}$ becomes in case $V_{c1} = V_{c2}$:

$$\sigma_{rel}^{'} = \left[\frac{(l_p - a)^5 + a^5}{(l_p - a)^5 - (5l_p - a)a^4}\right]^{V_{c1}=V_{c2}}. \quad (24)$$

2.2. Differential Capacitance

The differential capacitance is give by [33].

$$C = \frac{\partial Q_d}{\partial V_c}, \quad (25)$$

where

$$Q_d = q \times N_d \times l_p. \quad (26)$$

Here Q_d is the carrier due to donors in the depletion region; l_p is the width of the depletion region; q is the charge of the electron; V_c is the voltage contact measured in the interface of the metal semiconductor contact; and N_d is the density of background impurities.

Then we find:

$$C = q \times N_d \times \frac{\partial l_p}{\partial V_c}. \tag{27}$$

3. RESULTS AND DISCUSSION

The starting parameters for δ-MIGFET in GaAs are: $m^* = 0.067m_0$, ϵ_r =12.5, $N_{2d} = 7.5 \times 10^{12}\,\mathrm{cm}^{-2}$, $N_d = 1 \times 10^{18}\,\mathrm{cm}^{-3}$, $E_f = 0\,\mathrm{meV}$.

3.1. Case $V_{c1} \neq V_{c2}$

Figure 2 reports results of calculating the profile of the potential and sub-band energies with their envelope wave functions. We obtained the results using the Thomas Fermi model with $N_{2d} = 7.5 \times 10^{12}\,\mathrm{cm}^{-2}$, $V_{c1} = 500\,\mathrm{meV}$, $V_{c2} = 300\,\mathrm{meV}$, and the background impurities density is $N_d = 1 \times 10^{18}\,\mathrm{cm}^{-3}$, at $T = 0\,\mathrm{K}$. Here the n-type delta doped quantum-well is located at 300Å from the first and the second interface.

The dashed curve represents the obtained confining potential profile, and the solid curves represent the eigenvalues and eigenfunctions, where blue solid curve, red solid curve and green solid curve are the fundamental state eigenfunction, the second state eigenfunction and the third state eigenfunction, respectively.

Figure 2 represents an asymmetric profile of the potential because $V_{c1} \neq V_{c2}$, and it represents also eigenvalues, $E_0 = -155.6\,\mathrm{meV}$, $E_1 = -61.9\,\mathrm{meV}$ and $E_2 = -20.3\,\mathrm{meV}$ with the Fermi level taken close to the bottom of conduction band for the GaAs. The eigenfunctions and eigenvalues represent the starting point for transport phenomena calculations.

Figure 3 shows the relative mobility as a function of the first contact potential V_{c1} with $50\,\mathrm{meV} < V_{c1} < 650\,\mathrm{meV}$ from $N_{2d} = 7.5 \times 10^{12}\,\mathrm{cm}^{-2}$. Reference values are taken for $(V_{c1} = 0, V_{c2})$. The curves from bottom to top correspond to the second potential contact $V_{c2} = 50$, 100, 200, 300 and 400 meV, respectively.

The relative mobility (Figure 3) behaves in two forms. The first one is rising in a almost linear form when $V_{c2} \leq 300\,\mathrm{meV}$ and the second is rising in a parabolic form when $V_{c2} = 400\,\mathrm{meV}$ and $V_{c1} > 400\,\mathrm{meV}$.

We can see the difference in relative mobility between ($V_{c1} = 50\,\mathrm{meV}$, $V_{c2} = 50\,\mathrm{meV}$) and ($V_{c1} = 50\,\mathrm{meV}$, $V_{c2} = 400\,\mathrm{meV}$) and between ($V_{c1} = 650\,\mathrm{meV}$, $V_{c2} = 50\,\mathrm{meV}$) and ($V_{c1} = 650\,\mathrm{meV}$,

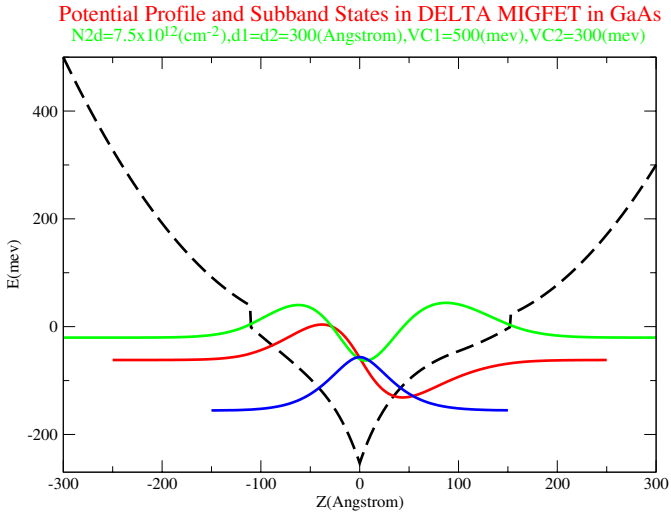

Figure 2. Conduction band, Eigenvalues and Eigenfunctions, Energies in meV for $V_{c1} = 500\,\text{meV}$, $V_{c2} = 300\,\text{meV}$, $N_{2d} = 7.5 \times 10^{12}\,\text{cm}^{-2}$, $d = 300\text{Å}$.

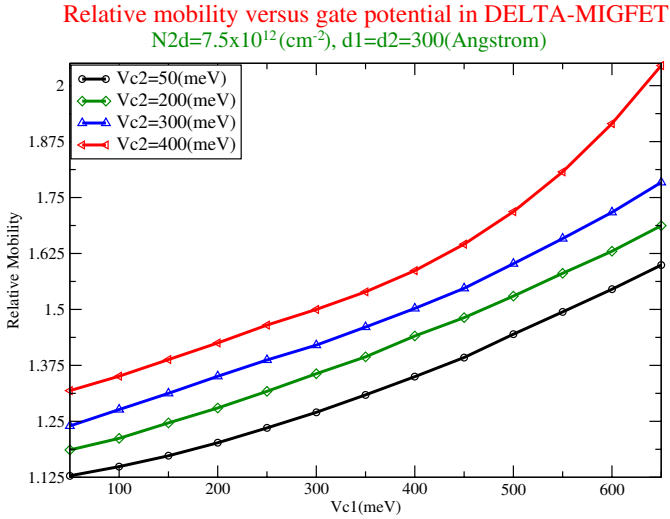

Figure 3. Relative mobility as a function of potential of contact V_{c1} (Correspond to the different value of V_{c2}) δ-MIGFET in GaAs for $N_{2d} = 7.5 \times 10^{12}\,\text{cm}^{-2}$, $d = 300\text{Å}$.

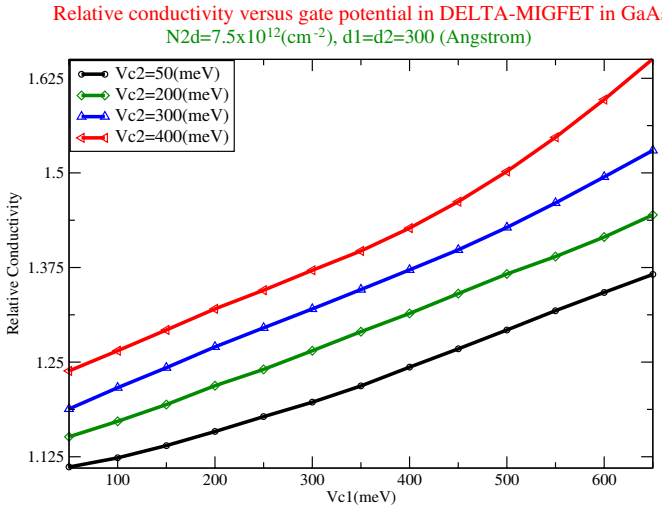

Figure 4. Relative Conductivity as a function of potential of contact V_{c1} (Correspond to the different value of V_{c2}) δ-MIGFET in GaAs for $N_{2d} = 7.5 \times 10^{12}\,\mathrm{cm}^{-2}$, $d = 300\mathring{\mathrm{A}}$.

$V_{c2} = 400\,\mathrm{meV}$). The value of mobility difference increases from 0.18 to 0.44, and it doubles.

Generally the mobility increases when increasing V_{c1} and V_{c2}. This could be explained by the fact that the electrons in quantum take more energy to move when the two potentials contacts increase.

Figure 4 shows the relative conductivity as a function of V_{c1} with $50\,\mathrm{meV} < V_{c1} < 650\,\mathrm{meV}$ for different values of $V_{c2} = 50$, 200, 300 and 400 meV. The relative conductivity rises when V_{c1} and V_{c2} are rising, and it has an almost linear behavior. In other words, the transconductance is almost flat. The same behavior was seen in Ultra-Thin Independent Double Gate MOSFET in Munteanu's work [13].

This comportment means that this electronic device δ-MIGFET has a good conductivity when the first and second potentials are increasing. On the other hand, as we saw before, this device has in general a lineal behavior, and this feature has a great importance in electronic systems when a stable transconductivity is desired.

3.2. Case $V_{c1} = V_{c2}$

Now we analyze the system, δ-MIGFET, in the particular and interesting case when $V_{c1} = V_{c2}$.

Figure 5 shows the potential profile (The dashed curve) when

$V_{c1} = V_{c2} = 500$ meV and wave functions (The solid curves) for $N_{2d} = 7.5 \times 10^{12}\,\mathrm{cm}^{-2}$. Where blue solid curve, red solid curve and green solid curve are the fundamental state eigenfunction, the second state eigenfunction and the third state eigenfunction, respectively.

The band structure can be seen, and the profile potentials are symmetrical. This is mainly due to the fact that the two potential contacts are equal. $V_{c1} = V_{c2} = 500\,\mathrm{meV}$ and inter distances between quantum-well and the interfaces are equal too.

Table 1 summarizes the results of the eigenvalues calculations in both cases $V_{c1} = 500\,\mathrm{meV}$, $V_{c2} = 300\,\mathrm{meV}$ and $V_{c1} = V_{c2} = 500\,\mathrm{meV}$. We adopt the transfer matrix method in order to calculate the eigenvalues [35–37].

We see in Table 1 the second potential influence V_{c2} on the energy

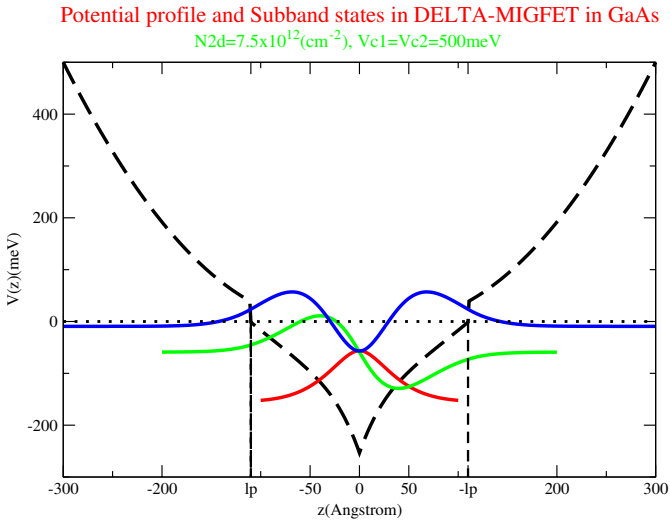

Figure 5. Electronic structure for δ-MIGFET in GaAs, where $V_{c1} = V_{c2} = 500\,\mathrm{meV}$ $N_{2d} = 7.5 \times 10^{12}\,\mathrm{cm}^{-2}$, $d = 300\text{Å}$.

Table 1. Energy levels (E_0, E_1, E_2) for different values of gate potential of V_{c2} and for ($V_{c1} = 500\,\mathrm{meV}$, $d = 300\text{Å}$, $N_{2d} = 7.5 \times 10^{12}\,\mathrm{cm}^{-2}$).

V_{c2}	$E_f - E_0$ **(meV)**	$E_f - E_1$ **(meV)**	$E_f - E_2$ **(meV)**
300 meV	155.6	61.9	20.3
500 meV	155.5	59.0	9.3

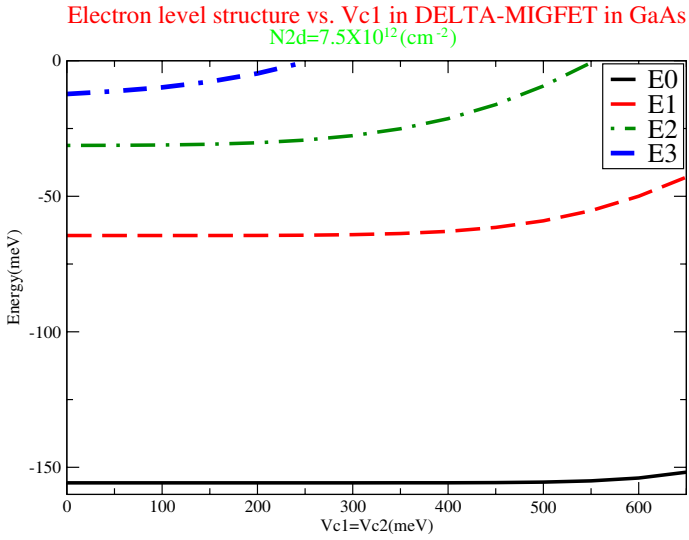

Figure 6. Electron level structure versus $V_{c1} = V_{c2}$ in δ-MIGFET in GaAs, where, $N_{2d} = 7.5 \times 10^{12}\,\mathrm{cm}^{-2}$, $d = 300$Å.

levels. The fundamental state does not feel the effects of V_{c2}, as $E_f - E_0 = 155.6\,\mathrm{meV}$ for $V_{c2} = 300\,\mathrm{meV}$ and $E_f - E_0 = 155.5\,\mathrm{meV}$ for $V_{c2} = 500\,\mathrm{meV}$.

In contrast, the superior levels feel the change of V_{c2}. Specially, the upper level decreases rapidly from $E_f - E_2 = 20.3\,\mathrm{meV}$ at $V_{c2} = 300\,\mathrm{meV}$ to $E_f - E_2 = 9.3\,\mathrm{meV}$ at $V_{c2} = 500\,\mathrm{meV}$.

In Figure 6, we represent the energy variation levels as a function of the voltage contact $V_{c1} = V_{c2}$. The fundamental state is almost stable at a value around $-155\,\mathrm{meV}$ when $V_{c1} < 550\,\mathrm{meV}$. In contrast, the superior energy levels feel the effect when the potential contacts grow. On the other hand, the potential contacts severely affect the superior levels. We observe that the number of levels decreases when increasing V_{c1}. If $V_{c1} < 250\,\mathrm{meV}$, we have 4 levels of energy. If $250\,\mathrm{meV} < V_{c1} < 550\,\mathrm{meV}$, we have 3 levels. Finally, if $550\,\mathrm{meV} < V_{c1}$ the level number is 2. This observation will help us to explain the transport phenomena.

Figure 7 gives the variation of the relative mobility as a function of the potential contacts when the device is operating in the symmetrical mode ($V_{c1} = V_{c2}$).

The solid curve presents the result achieved using the expression (11), and the dashed curve presents the result using the expression

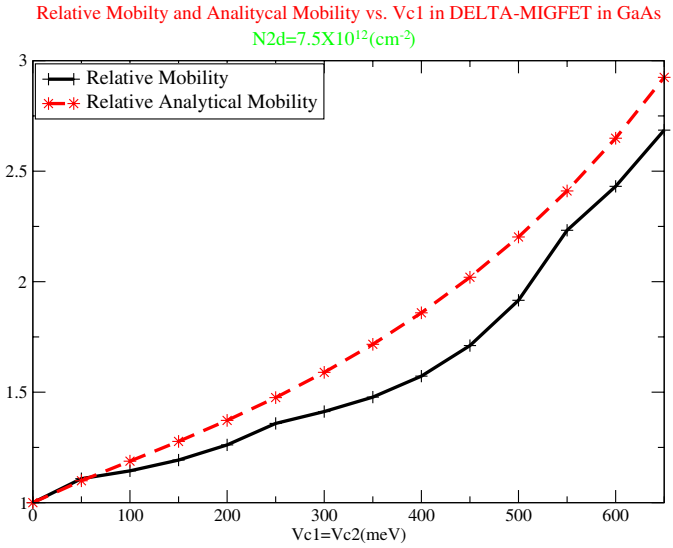

Figure 7. Relative Mobility as a function of gate potential V_{c1} ($V_{c1} = V_{c2}$) of δ-MIGFET in GaAs for $N_{2d} = 7.5 \times 10^{12}\,\mathrm{cm}^{-2}$, $d = 300\text{Å}$.

Table 2. Fluctuation percentage between both expressions of transport phenomenon for different values of gates potential, $V_{c1} = V_{c2}$, $d = 300\text{Å}$ and for $N_{2d} = 7.5 \times 10^{12}\,\mathrm{cm}^{-2}$.

$V_{c1} = V_{c2}$	200 **meV**	400 **meV**	600 **meV**
$\frac{\mu_{rel}-\mu'_{rel}}{\mu_{rel}} \times 100$	8.7	18	8.8
$\frac{\sigma_{rel}-\sigma'_{rel}}{\sigma_{rel}} \times 100$	4	10	4

follow (19).

The solid curve can be divided into three regions: the first in 50–250 meV, the second in 250–550 meV, and the third in 550–650 meV. We can explain this subdivision by the change in the number of quantum states in delta-quantum well in each region. Each interval can fit in a parabolic curve with a different bending.

In the case of the dashed curve, the relative analytical mobility behaves in the same way as the mobility for the first form. It increases in a parabolic way when V_{c1} is rising.

Table 2 presents the difference in the results between two ways of calculating the transport.

In the case of mobility, the difference does not exceed 8.7 percent at $V_{c1} = 200\,\text{meV}$ (In the first region). At $V_{c1} = 400\,\text{meV}$ (In the second region) the order is 18 percent, and in the last region $V_{c1} = 600\,\text{meV}$ is 8.8 percent. The fluctuation is due to the approach considered in the analytical mobility calculation. As we can see, the second form can perfectly predict the tendency of the mobility in the low potential $V_{c1} < 250\,\text{meV}$ and in the high potential $V_{c1} > 550\,\text{meV}$.

Figure 8 presents the behavior of the relative conductivity in the symmetric mode, as a function of gates potential. The dashed curve is the relative analytical conductivity using the expression (24). On the other hand, the solid curve is obtained using structure electronic results of the system.

Solid curve of the conductivity can be subdivided in three intervals: The first interval is when $V_{c1} < 250\,\text{meV}$; the second one is goes from 250 meV to 550 meV; and the last one is when 550 meV $< V_{c1}$. This subdivision is given by changing the number of states in each region.

Table 2 allows to compare the conductivity calculation between σ_{rel} and σ'_{rel} at some contact potential. We can see that the fluctuation at $V_{c1} = 200\,\text{meV}$ is 4 percent, at $V_{c1} = 400\,\text{meV}$ is 10 percent and at $V_{c1} = 600\,\text{meV}$ is 4 percent.

We can consider that the relative analytical conductivity σ'_{rel} is

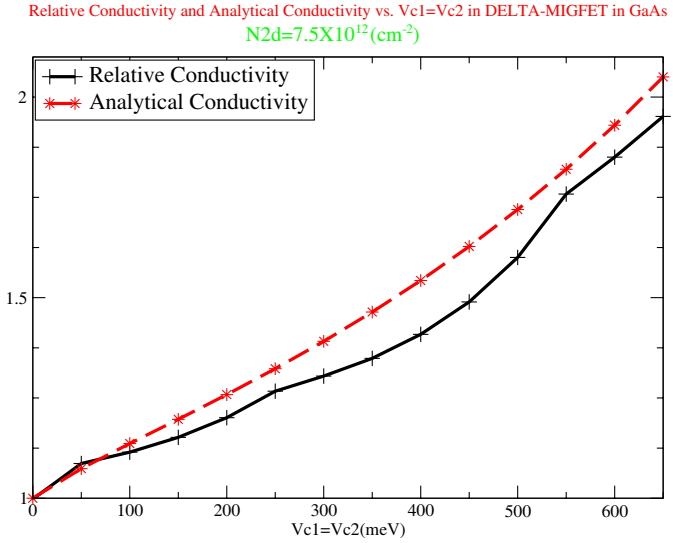

Figure 8. Relative Conductivity as a function of gate potential V_{c1} ($V_{c1} = V_{c2}$) of δ-MIGFET in GaAs for $N_{2d} = 7.5 \times 10^{12}\,\text{cm}^{-2}$, $d = 300\text{Å}$.

in accordance with σ_{rel}, and it is a good approximation of calculating the relative conductivity without calculating the electronic structure of this device.

Finally, as a first conclusion we can observe that the relative mobility and conductivity in the asymmetrical mode has better linearity than the relative mobility and conductivity in the symmetrical mode. The same remark was noted for transconductance in previous experimental work in a conventional MIGFET [11]. Also, we can conclude that the transport properties in both modes are almost doubled when the potentials V_{c1} and V_{c2} are maximum.

In conclusion, the analytical conductivity is a good and quick tool to calculate and get a good idea about the behavior of conductivity without calculating the eigenvalues or eigenfunctions.

In Figure 9, we see the variation of the analytical resistivity for different values of the bidimensional density of system. We see that this analytical quantity is decreasing in almost linear way when gate potential is increasing. If we compare the slope of the analytical resistivity among the four values of N_{2d} ($1\times10^{12}\,\mathrm{cm}^{-2}$, $2.5\times10^{12}\,\mathrm{cm}^{-2}$, $5\times10^{12}\,\mathrm{cm}^{-2}$ and $7.5\times10^{12}\,\mathrm{cm}^{-2}$) we observe that the slope grows.

It is clearly noted that the resistivity of the system rises with

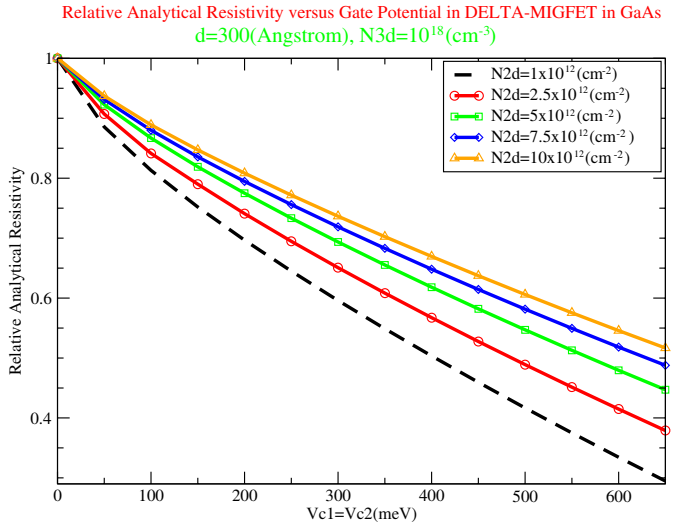

Figure 9. Relative analytical resistivity as a function of the voltage contact for different values of the two-dimensional impurity density, $N_{2d} = 7.5\times10^{12}\,\mathrm{cm}^{-2}, 5\times10^{12}\,\mathrm{cm}^{-2}, 2.5\times10^{12}\,\mathrm{cm}^{-2}$ and $1\times10^{12}\,\mathrm{cm}^{-2}$ in δ-MIGFET in GaAs.

increasing the bidimensional density in the delta doped. In this case the system is more resistive for $N_{2d} = 10 \times 10^{12}\,\mathrm{cm}^{-2}$ than the rest densities.

We conclude that the density in the well controls one of the most important electrical properties which is the resistivity.

In case that we improve the approximation made for the analytical transport quantity, another parameter which will appear is the background density, which controls also the resistivity.

In Figure 10, we observe the inverse square of the differential capacitance as a contact voltage function for different values of the two-dimensional impurity density, $N_{2d} = 7.5 \times 10^{12}\,\mathrm{cm}^{-2}$, $5 \times 10^{12}\,\mathrm{cm}^{-2}$, $2.5 \times 10^{12}\,\mathrm{cm}^{-2}$, $1 \times 10^{12}\,\mathrm{cm}^{-2}$ in δ-MIGFET, and in conventional MIGFET in GaAs. We observe, in Figure 10, that when we have an electronic localization, the slope of the curve for $N_{2d} = 7.5 \times 10^{12}\,\mathrm{cm}^{-2}$ is greater than the slope of the curve for $N_{2d} = 5 \times 10^{12}\,\mathrm{cm}^{-2}$, $N_{2d} = 2.5 \times 10^{12}\,\mathrm{cm}^{-2}$ and $N_{2d} = 1 \times 10^{12}\,\mathrm{cm}^{-2}$.

On the other hand, we see that the curvature of C^{-2} increases with the rising of δ doped well electronic density. This result is compatible with other works in δ-FET [24] and in ALD-FET [25].

In the case of the conventional MIGFET, where there is no

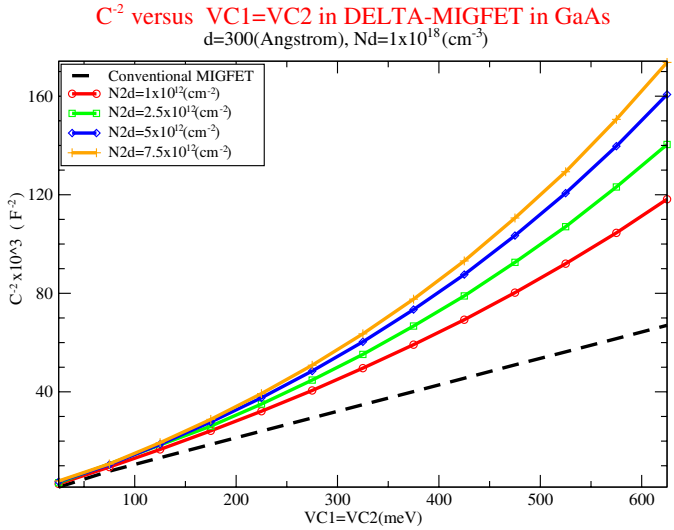

Figure 10. C^{-2} as a function of the voltage contact for different values of the two-dimensional impurity density, $N_{2d} = 7.5 \times 10^{12}\,\mathrm{cm}^{-2}, 5 \times 10^{12}\,\mathrm{cm}^{-2}, 2.5 \times 10^{12}\,\mathrm{cm}^{-2}, 1 \times 10^{12}\,\mathrm{cm}^{-2}$ in δ-MIGFET and in Conventional MIGFET in GaAs.

electronics confinement, we see straight line with the smallest slop. This straight line will be a reference when it is needed to know if there is or not a localization.

Also, if we try to determine, in a conventional way, the density background of impurities when electronic confinement exists, the concentration change measurement by this method will be less in real one.

We present in Figure 11 the bottom of the conduction channel in the function of background density and the contact potential of the two gates in the symmetric case ($V_{c1} = V_{c2}$).

We can observe in this figure two interesting dark areas. The upper dark area shows the conducting channel when the channel is open, which means that, for a given background density, the conduction channel does not feel the effects of contact potential of the two gates.

The dark area below represents a closed conducting channel when the potential of the conduction channel bottom is zero.

The two dark areas allow in these types of transistors to identify the digital operation mode of the system. In another way, when the conduction channel is open (dark area above) the transistor is saturated, and when the conduction channel is closed (dark area below) the transistor is blocked.

On the other hand, the intermediate region between the two dark areas predicts the alteration of the well bottom by the presence of the two Schottky barriers.

For a given background density N_d, this region will be determined by the following inequality $6.62 \times 10^{-16} N_d + 5\,\text{meV} \leq V_c \leq -0.027 \times (10^{-16} N_d - 259)^2 + 2 \times 10^3\,\text{meV}$. At last, in this intermediate region, we can see that the transistor can operate in analogue mode.

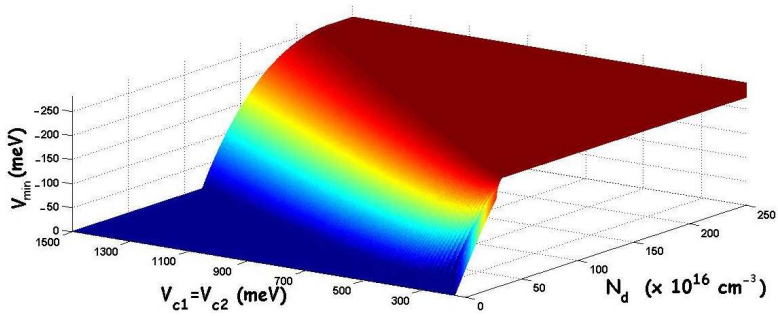

Figure 11. Bottom of the n-type delta-doped well $V_{\min}$ vs. N_d and $V_{c1} = V_{c2}$ for $N_{2d} = 7.5\times$, $10^{12}\,\text{cm}^{-2}$ in δ-MIGFET in GaAs.

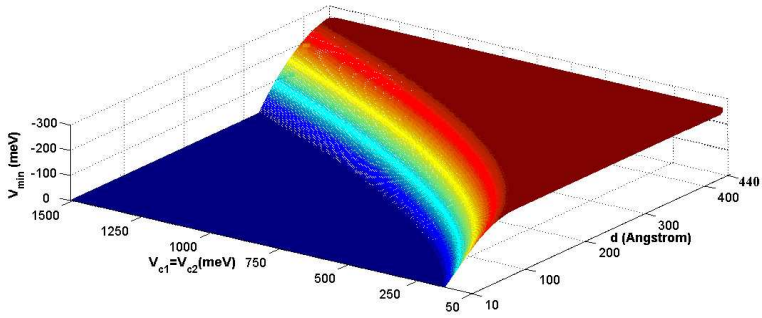

Figure 12. Bottom of the n-type delta-doped well ($V_{\min}$) *vs.* d and $V_{c1} = V_{c2}$ for $N_{2d} = 7.5\times$, $10^{12}\,\mathrm{cm}^{-2}$ in δ-MIGFET in GaAs.

In Figure 12, we also present the bottom of the conduction channel in the function of the distance at which the n-type delta-doped well is positioned and the contact potential of the two gates in the symmetric case ($V_{c1} = V_{c2}$). From the figure we can infer the analogical mode, where $0.0038 \times (d - 216)^2 + 192.8\,\mathrm{meV} \leq V_c \leq 0.007 \times (d + 16)^2 - 16.5\,\mathrm{meV}$.

4. CONCLUSIONS

This device is characterized mainly by the increasing lineal function in the mobility and the conductivity for both modes. It was found that the conductivity in this device has better linearity in the asymmetrical mode than in the symmetrical mode as occurs in experimental results of such systems. These features have a great importance in microelectronics industry when linearity is desired.

The analytical transport is a good and quick qualitative tool for studying the behavior of conductivity and mobility; it can be applied to other systems. It is possible to improve the relative analytical transport if we use a better approximation when calculating this quantity.

The tools presented in this work are helpful to observe at least a qualitative way for microelectronics industry, to know the behavior of the resistivity and capacity, to specify the different regions of operation modes in the device or to determinate if there is or not electronics confinement.

Thanks to the interesting transport and electrical properties of δ-MIGFET, this device may be another alternative and concurrent for the transistors used today.

ACKNOWLEDGMENT

O. Ou acknowledges partial support from CONACyT project No. 2005/51458 and PIFCA-190. L. M. G-S acknowledges UAEM (State Autonomous University of Morelos, at Cuernavaca, Mexico) for support.

REFERENCES

1. Kimura, S., D. Hisamoto, and N. Sugii, "Prospect of Si semiconductor devices in nanometer era," *Hitachi Review*, Vol. 54, No. 1, 2–8, 2005.
2. Munteanu, D. and J. L. Autran, "3-D simulation analysis of bipolar amplification in planar double-gate and FinFET with independent gates," *IEEE Trans. Nucl. Sci.*, Vol. 56, No. 4, 2083–2090, 2009.
3. Giroldo, Jr., J. and M. Bellodi, "Drain leakage current in MuGFETs at high temperatures," *ECS Trans.*, Vol. 28, No. 4, 1169. 2010.
4. Sampedro, C., F. Gámiz, A. Godoy, R. Valín, A. García-Loureiro, and F. G. Ruiz, "Multi-subband Monte Carlo study of device orientation effects in ultra-short channel DGSOI," *Solid-State Electron.*, Vol. 54, No. 2, 131–136, 2010.
5. Mikki, S. M. and A. A. Kishk, "A symmetry-based formalism for the electrodynamics of nanotubes," *Progress In Electromagnetics Research*, Vol. 86, 111–134, 2008.
6. Mathew, L., Y. Du, A. V.-Y. Thean, M. Sadd, A. Vandooren, C. Parker, T. Stephens, R. Mora, R. Rai, M. Zavala, D. Sing, S. Kalpat, J. Hughes, R. Shimer, S. Jallepalli, G. Workman, W. Zhang, J. G. Fossum, B. E. White, B.-Y. Nguyen, and J. Mogab, "CMOS vertical multiple independent gate field effect transistor (MIGFET)," *IEEE SOI Conference*, 187–189, 2004.
7. Mathew, L., Y. Du, S. Kaipat, M. Sadd, M. Zavala, T. Stephens, R. Mora, R. Rai, et al., "Multiple independent gate field effect transistor (MIGFET) multi-Fin RF mixer architecture, three independent gates (MIGFET-T) operation and temperature characteristics," *IEEE VLSI Technology*, 200–201, 2005.
8. Baviskar, P., S. Jain, and P. Vinchurkar, "Nano scale soi mosfet structures and study of performance factors," *Int. J. Comput. Appl.*, Vol. 1, No. 28, 2010.
9. Jagadesh Kumar, M. and G. V. Reddy, "Diminished short channel effects in nanoscale double-gate silicon-on-insulator metal-oxide-

semiconductor field-effect-transistors due to induced back-gate step potential," *Jpn. J. Appl. Phys.*, Vol. 44, No. 9A, 6508–6509, 2005.

10. Hu, G., R. Liu, Z. Qiu, L. Wang, and T. Tang, "Quantum mechanical effects on the threshold voltage of double-gate metal-oxide-semiconductor field-effect transistors," *Jpn. J. Appl. Phys.*, Vol. 49, 034001, 2010.
11. Gong, J. and P. C. H. Chan, "Linearity study of multiple independent gate field effect transistor (MIGFET) under symmetric and asymmetric operations," *Solid-State Electron.*, Vol. 52, No. 2, 259–263, 2008.
12. Hamed, H. F. A., S. Kaya, and J. A. Starzyk, "Use of nano-scale double-gate MOSFETs in low-power tunable current mode analog circuits," *Analog. Integr. Circ. S.*, Vol. 54, No. 3, 211–217, 2008.
13. Munteanu, D., M. Moreau, and J. L. Autran, "A compact model for the ballistic subthreshold current in ultra-thin independent double-gate MOSFETs," *Mol. Simulat.*, Vol. 35, No. 6, 491–497, 2009.
14. Jiménez, D., J. J. Sáenz, B. Iñíquez, J. Suñé, L. F. Marsal, and J. Pallarès, "Unified compact model for the ballistic quantum wire and quantum well metal-oxide-semiconductor field-effect-transistor," *J. Appl. Phys.*, Vol. 94, No. 2, 1061–1068, 2003.
15. Moreno, E., J. B. Roldán, F. G. Ruiz, D. Barrera, A. Godoy, and F. Gámiz, "An analytical model for square GAA MOSFETs including quantum effects," *Solid-State Electron.*, Vol. 54, No. 11, 1463–1469, 2010.
16. Chaisantikulwat, W., M. Mouis, G. Ghibaudo, S. Cristoloveanu, J. Widiez, M. Vinet, and S. Deleonibus, "Experimental evidence of mobility enhancement in short-channel ultra-thin body double-gate MOSFETs by magnetoresistance technique," *Solid-State Electron.*, Vol. 51, No. 11–12, 1494–1499, 2007.
17. Shrivastava, M., M. S. Baghini, A. B. Sachid, D. K. Sharma, and V. R. Rao, "A novel and robust approach for common mode feedback using IDDG FinFET," *IEEE Trans. Electron Devices*, Vol. 55, No. 11, 3274–3282, 2008.
18. Nakajima, S., N. Kuwata, N. Shiga, K. Otobe, K. Matsuzaki, T. Sekiguchi, and H. Hayashi, "Characterization of double pulse-doped channel GaAs MESFETs," *IEEE Trans. Electron Devices*, Vol. 14, No. 3, 146–148, 1993.
19. Roberts, J. M., J. J. Harris, N. J. Woods, and M. Hopkinson, "Investigation of delta-doped quantum wells for power FET applications," *Superlattice Microst.*, Vol. 23, No. 2, 187–190, 1998.

20. Kao, M. J., W. C. Hsu, R. T. Hsu, Y. H. Wu, and T. Y. Lin, "Characteristics of graded-like multiple-delta-doped GaAs field effect transistors," *Appl. phys. Lett.*, Vol. 66, No. 19, 2505, 1995.
21. Oubram, O. and L. M. Gaggero-Sager, "Transport properties of delta doped field effect transistor," *Progress In Electromagnetics Research Letters*, Vol. 2, 81–87, 2008.
22. Gaggero-Sager, L. M. and R. Pérez-Alvarez, "A simple model for delta-doped field-effect transistor electronic states," *J. Appl. Phys.*, Vol. 78, No. 7, 4566–4569, 1995.
23. Oubram, O. and L. M. Gaggero-Sager, "Relative mobility and relative conductivity in ALD-FET (atomic layer doped-field effect transistor) in GaAs," *PIERS Proceedings*, 1186–1190, Beijing, China, March 23–27, 2009.
24. Martínez-Orazco, J. C., L. M. Gaggero-Sager, and S. J. Vlaev, "Differential capacitance as a method of determining the presence of a quasi-electronic gas bidemensional," *Solid-State Electron.*, Vol. 48, No. 12, 2277–2280, 2004.
25. Martínez-Orazco, J. C., L. M. Gaggero-Sager, and S. J. Vlaev, "A Simple model for diffential capacitance profile in the atomic layer doped field effect transistor (ALD-FET) in GaAs," *Mat. Sci. Eng. B-solid*, Vol. 84, No. 3, 155–158, 2001.
26. Chakhnakia, Z. D., L. V. Khvedelidze, N. P. Khuchua, R. G. Melkadze, G. Peradze, and T. B. Sakharova, "AlGaAs-GaAs heterostructure δ-doped field effect transistor (δ-FET)," *Proc. SPIE*, Vol. 5401, 354–360, 2004.
27. Bènière, F., R. Chaplain, M. Gauneau, V. Redd, and A. Régrény, "Delta-doping in diffusion studies," *J. Phys. III France 3*, Vol. 3, No. 12, 2165–2171, 1993.
28. Schubert, E. F., A. Fischer, and K. Ploog, "The delta-doped field-effect transistor (δ-FET)," *IEEE Trans. Electron Devices*, Vol. 33, No. 5, 625–632, 1986.
29. Chen, X. and B. Nabet, "A closed-form expression to analyze electronic properties in delta-doped heterostructures," *Solid-State Electron.*, Vol. 48, No. 12, 2321–2327, 2004.
30. Ozturk, E., "Effect of magnetic field on a p-type d-doped GaAs layer," *Chinese Phys. Lett.*, Vol. 27, No. 7, 077302, 2010.
31. Ozturk, E., "Optical intersubband transitions in double Si d-doped GaAs under an applied magnetic field," *Superlattices and Microstructures*, Vol. 46, No. 5, 752–759 2009.
32. Ozturk, E., M. K. Bahar, and I. Sokmen, "Subband structure of p-type δ-doped GaAs as dependent on the acceptor concentration

and the layer thickness," *Eur. Phys. J. Appl. Phys.*, Vol. 41, No. 3, 195–200, 2008.

33. Rhoderick, E. H. and R. H. Williams, *Metal-semiconductor Contacts*, Clarendon Press, Oxford, 1988.
34. Rodríguez-Vargas, I., L. M. Gaggero-Sager, and V. R. Velasco, "Thomas-Fermi-Dirac theory of the hole gas of a double p-type delta-doped GaAs quantum wells," *Surf. Sci.*, Vol. 537, No. 1, 75–83, 2003.
35. Samuel, E. P. and D. S. Patil, "Analysis of wavefunction distribution in quantum well biased laser diode using transfer matrix method," *Progress In Electromagnetics Research Letters*, Vol. 1, 119–128, 2008.
36. Liu, C.-C., Y.-H. Chang, T.-J. Yang, and C.-J. Wu, "Narrowband filter in a heterostructured multilayer containing ultrathin metalic films," *Progress In Electromagnetics Research*, Vol. 96, 329–346, 2009.
37. Talele, K. and D. S. Patil, "Analysis of wave function, energy and transmission coefficients in GaN/AlGaN superlattice nanostructures," *Progress In Electromagnetics Research*, Vol. 81, 237–252, 2008.